J Mater Sci (2008) 43:609–613
DOI 10.1007/s10853-007-1778-4

5TH BRAZILIAN MRS MEETING

Effect of processing conditions on the nucleation and growth of indium-tin-oxide nanowires made by pulsed laser ablation

Raluca Savu · Ednan Joanni

Received: 30 January 2007 / Accepted: 13 April 2007 / Published online: 22 June 2007

Abstract Indium–tin oxide nanowires were deposited by excimer laser ablation onto catalyst-free oxidized silicon substrates at a low temperature of 500 °C in a nitrogen atmosphere. The nanowires have branches with spheres at the tips, indicating a vapor–liquid–solid (VLS) growth. The deposition time and pressure have a strong influence on the areal density and length of the nanowires. At the earlier stages of growth, lower pressures promote a larger number of nucleation centers. With the increase in deposition time, both the number and length of the wires increase up to an areal density of about 70 wires/μm^2. After this point all the material arriving at the substrate is used for lengthening the existing wires and their branches. The nanowires present the single-crystalline cubic bixbyite structure of indium oxide, oriented in the ⟨100⟩ direction. These structures have potential applications in electrical and optical nanoscale devices.

Introduction

Recent developments in nanotechnology have led to the synthesis and characterization of a variety of nanostructures, such as nanowires, nanorods, nanotubes, and nanopyramids. These nanometer-scale structures possess enhanced optical and electrical characteristics due to quantum confinement effects, as well as high surface-to-volume ratios [1–4]. Crucial factors in the synthesis of nanowires are the control of morphology, size uniformity, growth direction, and dopant distribution within the nanostructures, as these structural parameters will ultimately dictate their functionality [3].

Indium-doped tin oxide (ITO) is a transparent conducting oxide material that has been used in a variety of applications such as optoelectronic devices, solar cells, liquid crystal displays, and sensors. Over the past decades, much research effort has been spent on the synthesis of ITO thin films [5–9]. More recently, research has been conducted on pure or tin-doped indium oxide nanostructures (predominantly nanowires) by both physical and chemical methods for potential applications in high-sensitivity sensor, optoelectronic, field-emission, electronic, and memory devices [10–16].

The most common growth mode for nanowires made by vapor deposition methods is the so-called vapor–liquid–solid (VLS) mechanism. According to this mechanism, the nanowires grow by precipitation from droplets of molten material present on the heated substrate surface [1, 16–19]. The catalyst-assisted nucleation and growth of nanowires by the VLS mechanism were modeled in terms of thermodynamic and kinetic variables and compared with experimental results for the Fe–Si, Au–Si, and Ga–Ge systems [18–20]. The theoretical treatment of the problem gets more complicated in the case of multi-element nanowires and metallic oxides.

The initial stages of growth for nanowires formed without a catalyst (nanoparticles or thin layers) play a very important role due to the effect of these initial conditions over the morphology, size, orientation, and number density

R. Savu · E. Joanni
INESC-Porto, Rua do Campo Alegre 687, 4169-007 Porto, Portugal

E. Joanni
Departamento de Física, Universidade de Trás-os-Montes e Alto Douro, 5001-911 Vila Real, Portugal

R. Savu (✉)
Instituto de Química, Universidade Estadual Paulista - UNESP, Rua Francisco Degni s/n, 14800-900 Araraquara, SP, Brazil
e-mail: raluk1978@yahoo.com

of wires on the substrate. In this work we report the growth of ITO nanowires by laser ablation on catalyst-free silicon substrates at a relatively low substrate temperature. The influence of deposition conditions over the nucleation and initial stages of growth were investigated.

Experimental procedure

ITO nanowires were deposited by laser ablation onto catalyst-free oxidized silicon substrates using a ceramic target having a $(In_2O_3)_{0.9}(SnO_2)_{0.1}$ composition. A KrF laser beam, with a 10 Hz frequency, was focused on the target to a spot size of 0.2 cm^2 and an energy of 130 mJ for all experiments, keeping also constant a 4 cm target-substrate distance. The growth times were 4, 8, and 20 min. Before each deposition, the chamber was evacuated to at least 10^{-5} Pa in order to avoid contamination by residual gases. After the substrate temperature reached 500 °C, pure nitrogen was introduced in the chamber until the desired pressures of 50 or 100 Pa. A longer deposition was also performed (60 min) at 100 Pa N_2 pressure. The samples were cooled in the same atmosphere and pressure used for the deposition until the substrate reached a temperature below 100 °C.

X-ray diffraction (X-ray) scans were performed in order to assess the crystal structure of the nanostructures and their orientation (Rigaku D/max, Siemens D5000). The nucleation stage, the morphology and the growth mechanism of the nanostructures were studied by field emission scanning electron microscopy (FE-SEM, Hitachi, S-4100). High-resolution transmission electron microscopy (HR-TEM, Phillips CM200), energy dispersive spectroscopy (EDS), and selected area electron diffraction (SAED) were performed on individual nanowires in order to determine the growth direction, chemical composition and interplanar distance.

Results and discussion

Figure 1 presents high-resolution FE-SEM images of substrate surfaces and cross-sections for the samples deposited at 50 and 100 Pa for 4, 8, and 20 min, respectively. The misaligned, detached or broken needles in the images are a consequence of breaking the substrates for cross-sectional analysis. In the initial stages of growth the substrate is covered by a thin dense layer consisting of small grains (approximately 20 nm) without any preferential orientation with nanowires protruding from this film. After 4 min deposition (Fig. 1a, b), the wires are very short and a big effect of the deposition pressure on the number of nucleation centers can be observed. For this reason, at 100 Pa (Fig. 1b) the nanowires are not yet evenly distributed over the substrate, having no uniformity in sizes when compared to the sample made at 50 Pa (Fig. 1a) were the nanowires have more uniform sizes and distribution. This can be

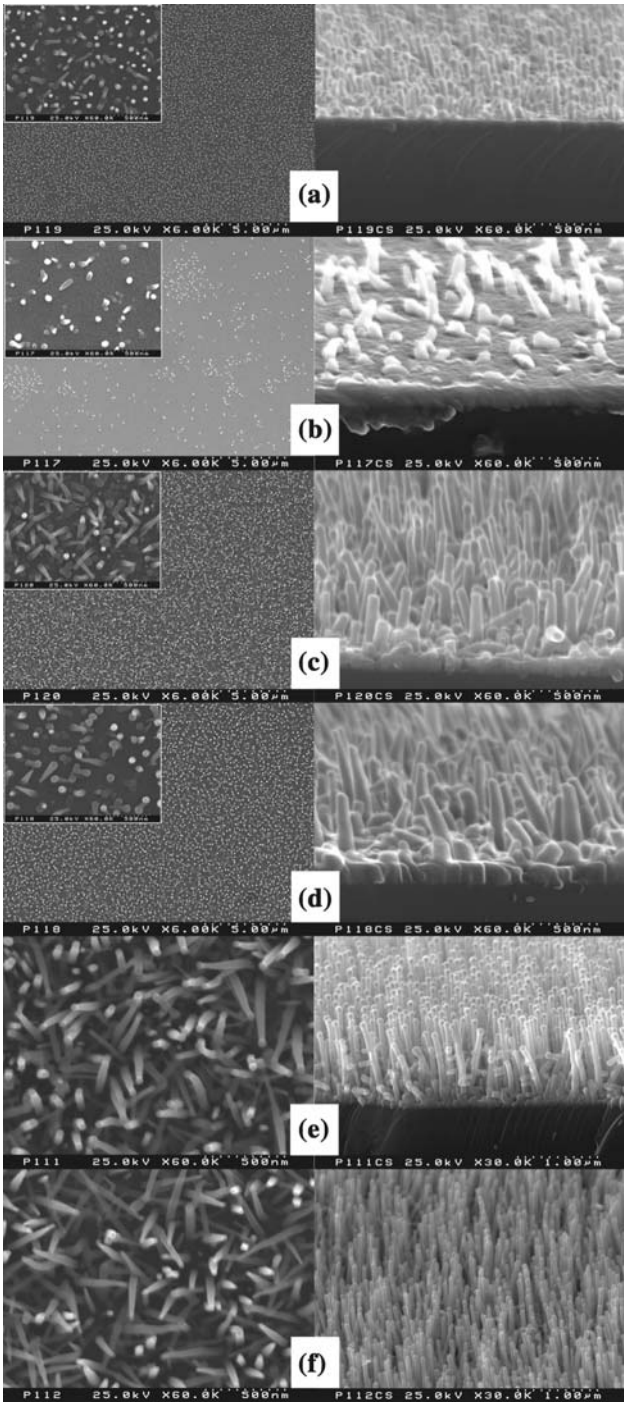

Fig. 1 FE-SEM surface and tilted cross-section images of films deposited at 50 Pa for 4 min (**a**), 8 min (**c**), and 20 min (**e**) and at 100 Pa for 4 min (**b**), 8 min (**d**), and 20 min (**f**)

explained by the smaller amount of liquid material generated at higher deposition pressure. At 500 °C the materials present in the liquid state can only be metallic tin and indium whose formation is favored by the lack of oxygen in the deposition atmosphere. With longer deposition times (8 and 20 min, Fig. 1c, d and e, f, respectively) the wires increase in length and their distribution across the substrate surface becomes similar for both pressures. One can also observe, in Fig. 1e, that for 50 Pa and 20 min deposition time the needles have branches and balls in the tips due to the higher amount of molten material present at lower pressure. This is also a strong indication of the VLS growth mechanism.

The degree of coverage of the substrates as a function of deposition time, measured by counting the nanowires on the SEM pictures is shown in Fig. 2. The higher nucleation rate at lower deposition pressure is clearly visible for the shortest deposition time. The nucleation rate for 50 Pa is high at the beginning with tendency to stabilize after 8 min deposition compared with 100 Pa where the rate increases almost linearly. As the deposition progresses, the number of wires per square micron increases for both pressures but there is a tendency for saturation, with the density of wires getting similar (around 70 wires/μm^2) for deposition times of 20 min. This is related to the maximum distance for material diffusion at the substrate temperature used in these experiments. Once the spacing between the wires becomes smaller than this maximum diffusion distance the new material arriving at the substrate is used for growing the existing wires and their branches, so the density of wires for a given substrate area tends to become constant. The curves on the graph were drawn assuming an asymptotic growth and according to this trend the maximum density of nanowires is almost reached after 20 min deposition, confirming our observations.

In order to assess the long time evolution of growth, a 60 min deposition at 100 Pa was performed. The cross-section image of this sample (Fig. 3) shows that after the maximum density of nanowires at the substrate is achieved, the new material arriving is used up for increasing the length of the wires. In other words, the result of an extended deposition time is not a dense array of short wires, but a sample with long wires, as predicted from the trends shown in Fig. 2. The wires have lengths around 4.5 μm with thicknesses of approximately 100 nm at the base and 70 nm at the tip.

X-ray diffraction scans were performed in order to assess the crystal structure of the nanowires and their orientation (Rigaku D/max, Siemens D5000). Figure 4 shows the diffraction patterns of the target as well as of the films deposited at 100 Pa (very similar diffraction patterns were also obtained for 50 Pa deposition pressure). Even though the X-ray diffraction pattern of the

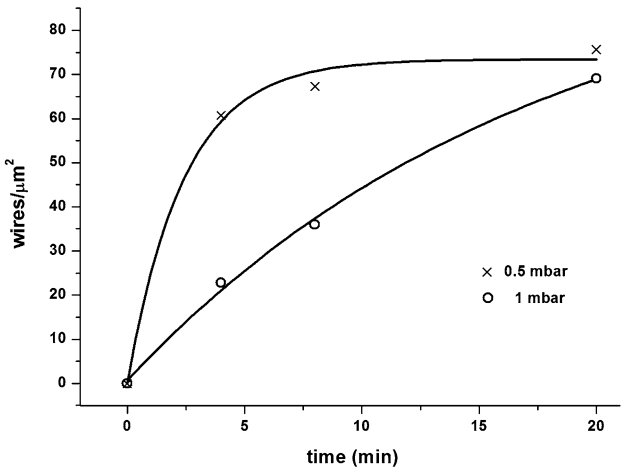

Fig. 2 Number of wires per area of substrate, for the used pressures, as a function of deposition time

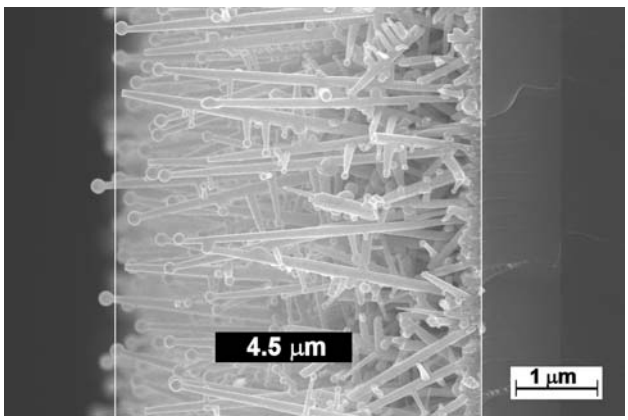

Fig. 3 FE-SEM cross-section image of the sample deposited at 100 Pa for 60 min

target shows traces of tin oxide, the samples exhibit peaks only from the cubic (bixbyite) structure of indium oxide, indicating that the tin is in solid solution and no incorporation of nitrogen occurred, as expected from the relatively low deposition temperature. The signal from the thin dense layer of small grains covering the substrates, discussed in the SEM analysis, is always present in the X-ray graphs. This is established by the occurrence of the three most intense peaks from ITO in all the samples, even though their relative intensities differ from those of the target.

The (400) growth direction of the wires can already be observed for the samples made with 4 min deposition time, even though the peaks have a very low intensity due to the small number of needles, as previously observed in the SEM images. Moreover, comparing the diffraction patterns

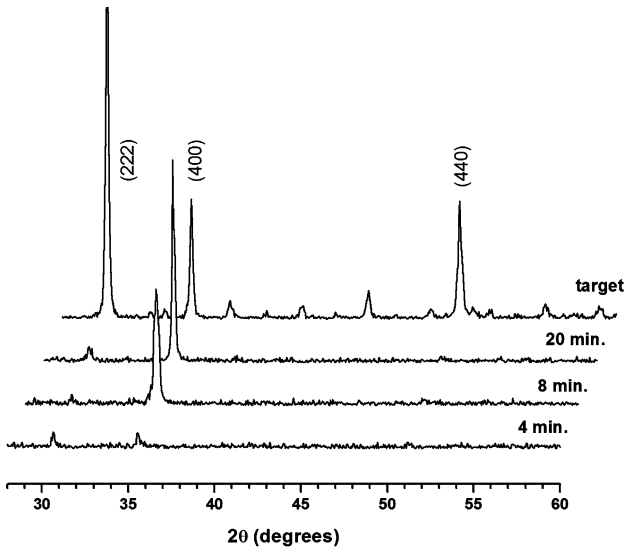

Fig. 4 X-ray diffraction patterns of the target and of the samples obtained at 100 Pa deposition pressure

from the target and the samples, the tendency for (400) growth of the nanowires is easily noticed, since this is the only peak whose intensity increases with deposition time. For the samples deposited for 8 and 20 min, the X-ray graphs exhibit strong (400) orientation, due to the higher degree of coverage of the substrate by the nanowires, confirming the SEM observations and counting measurements. The strong (400) orientation of the nanowires reflects a highly anisotropic crystalline growth and a good degree of alignment, perpendicular to the substrate.

Individual nanowires taken from the samples grown for 20 min were studied by HR-TEM and selected area electron diffraction (SAED) analysis (Fig. 5). Figure 5a shows a needle obtained at 100 Pa with a sphere on the tip, typical for a nanostructure formed by the VLS growth mechanism. No grain boundaries can be seen in the wire, confirming its single-crystalline structure, as expected from a VLS grown crystal. The wire is faceted, with a square cross-section, reflecting the cubic structure of indium oxide. Figure 5b exhibits a high-resolution TEM image of a wire formed at 50 Pa with an inset of the SAED pattern. In the HR-TEM image one can observe the interface between the sphere and the needle, the discrepancy in the crystalline structures being due to the different concentrations of tin detected by EDS, with the spheres having a very high tin content. The interplanar distance, measured as approximately 0.52 nm is characteristic of the 200 interplanar spacing for indium oxide. The SAED pattern taken perpendicular to the long axis of the nanowire is consistent with the indexed patterns from the indium oxide cubic structure with ⟨100⟩ growth direction.

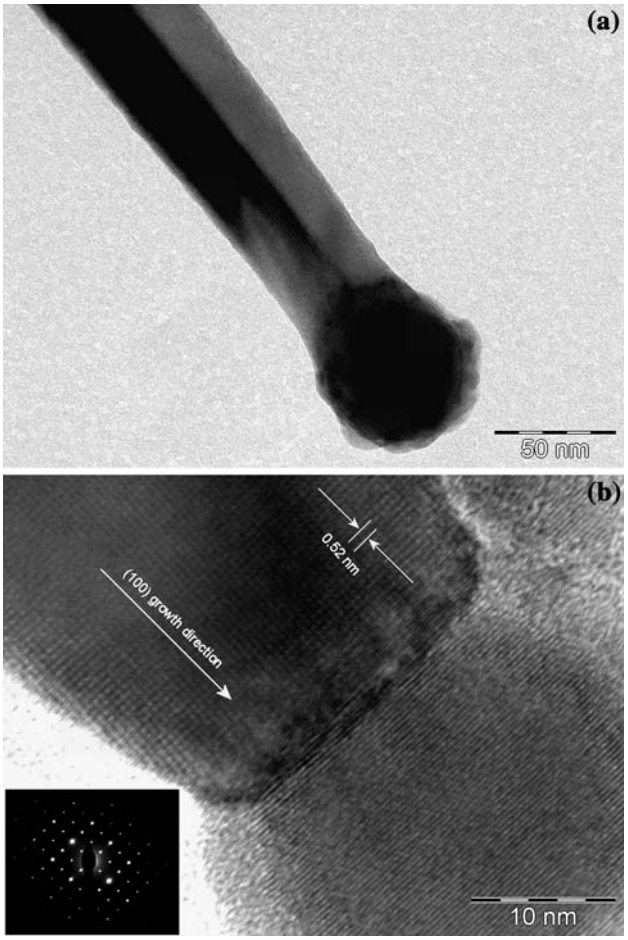

Fig. 5 HR-TEM images of individual nanowires broken from the samples grown at 100 Pa (**a**) and 50 Pa (**b**) for 20 min; the inset shows a selected area electron diffraction pattern (SAED) taken perpendicular to the long axis of the needle

Conclusions

In conclusion, we succeeded to synthesize ITO nanowires by excimer laser ablation of an oxide target onto catalyst-free silicon substrates in a nitrogen atmosphere. The wires are monocrystalline and grow perpendicular to the substrate along the ⟨100⟩ direction.

The deposition time and pressure have a strong influence on the areal density and length of the nanowires. As the deposition time increases, both the number and length of the wires increase, until a maximum density (which for our conditions is around 70 wires/μm^2) is achieved. After this point all the material arriving at the substrate is used for lengthening the existing wires and their branches.

At low pressure a large amount of liquid is formed during deposition, promoting the VLS growth of branched nanowires with spheres at the tips. As the deposition pressure increases, the amount of liquid phase decreases and the nanowires have fewer branches. The effect of

pressure is particularly important at the earlier stages of growth, with lower pressures favoring the formation of a larger number of nucleation centers.

These nanostructures have potential applications in field-emission displays, gas sensors, solar cells, photodetectors, and other nanoscale devices.

Acknowledgement We would like to acknowledge the help of Prof. Faramarz Farahi from UNC at Charlotte on parts of the FE-SEM characterization.

References

1. Rao CNR, Deepak FL, Gundiah G, Govindaraj A (2003) Prog Solid State Chem 31:5
2. Nguyen P, Ng HT, Yamada T, Smith MK, Li J, Han J, Meyyappan M (2004) Nano Lett 4:651
3. Law M, Goldberger J, Yang P (2004) Annu Rev Mater Res 34:83
4. Xia Y, Yang P, Sun Y, Wu Y, Mayers B, Gates B, Yin Y, Kim F, Yan H (2003) Adv Mater 15:353
5. Tahar RBH, Ban T, Ohya Y, Takahashi Y (1998) J Appl Phys 83:2631
6. Savu R, Joanni E (2006) Mater Sci Forum 514–516:1161
7. Ederth J, Heszler P, Hultaker A, Niklasson GA, Granqvist CG (2003) Thin Solid Films 445:199
8. Reddy VS, Das K, Dhar A, Ray SK (2006) Semicond Sci Technol 21:1747
9. Morales-Paliza MA, Haglund RF Jr, Feldman LC (2002) Appl Phys Lett 80:3757
10. Kim HW, Kim NH, Lee C (2005) Appl Phys A 81:1135
11. Wan Q, Wei M, Zhi D, MacManus-Driscoll JL, Blamire MG (2006) Adv Mater 18:234
12. Limmer SJ, Cruz SV, Cao GZ (2004) Appl Phys A 79:421
13. Liang YX, Li SQ, Nie L, Wang YG, Wang TH (2006) Appl Phys Lett 88:193119-1
14. Wan Q, Feng P, Wang TH (2006) Appl Phys Lett 89:123102-1
15. Yu D, Wang D, Yu W, Qian Y (2003) Mater Lett 58:84
16. Chen YQ, Jiang J, Wang B, Hou JG (2004) J Phys D: Appl Phys 37:3319
17. Savu R, Joanni E (2006) Scr Mater 55:979
18. Liu QX, Wang CX, Xu NS, Yang GW (2005) Phys Rev B 72:085417–1
19. Kwon SJ, Park JG (2006) J Phys: Condens Matter 18:3875
20. Chandrasekaran H, Sumanasekara GU, Sunkara MK (2006) J Phys Chem B 110:18351